



Battery cell arrangement and heat transfer fluid effects on the parasitic power consumption and the cell temperature distribution in a hybrid electric vehicle

Sungjin Park ^{a,*}, Dohoy Jung ^{b,1}

^a Department of Mechanical and System Design Engineering, Hongik University, 94 Wausan-Ro, Mapo-Gu, Seoul 121-791, Republic of Korea

^b Department of Mechanical Engineering, The University of Michigan-Dearborn, 4901 Evergreen Road, Dearborn, MI 48128, USA

HIGHLIGHTS

- The design and fluid type effects of the BTMS are investigated using numerical model.
- A wide battery module with a small cell to cell gap is desirable for the air type BTMS.
- A narrow battery module with a small gap is desirable for a liquid type BTMS.
- Fluid types and design should be selected depending on the heat load of the battery pack.

ARTICLE INFO

Article history:

Received 27 August 2012

Received in revised form

12 November 2012

Accepted 14 November 2012

Available online 23 November 2012

Keywords:

Battery thermal management system

Hybrid electric vehicle

Numerical modeling

Battery cell arrangement

Air type

Liquid type

ABSTRACT

Computationally efficient numerical models of battery cooling systems are developed and the effects of the battery cell arrangement and the heat transfer fluid (HTF) type on the cooling performance and the parasitic power consumption of the system are investigated. A one-dimensional heat conduction model of a cylindrical battery cell is developed using a finite difference method for the cell temperature prediction and a battery module model is developed to predict the cell to cell temperature variation and the power consumption of the systems depending on the design of battery module and operating conditions. The analysis of the battery thermal management system (BTMS) design by using the numerical model is conducted for air and liquid type BTMSs. From the numerical analysis, it is found that a wide battery module with a small cell to cell gap is desirable for the air type BTMS while a narrow battery module with a small gap is desirable for a liquid type BTMS. The results also show that the air type BTMS consumes much more power compared with the liquid type BTMS especially for high heat load condition. However, under low heat load conditions, the power consumption of the air type BTMS is acceptable considering its advantages over the liquid type BTMS.

© 2012 Elsevier B.V. All rights reserved.

1. Introduction

The battery operating temperature in hybrid electric vehicles (HEVs) affects the electrochemical reactions, charging and discharging efficiencies, durability, and reliability of the battery and eventually round trip efficiency, charge acceptance, safety, reliability, and the life cycle of a vehicle [1]. Better performance of a typical Li-ion battery is expected to perform better at the temperature range of 20 °C and 40 °C. At higher temperatures, the internal resistance decreases, the discharge voltage increases and, as a result, the ampere hour capacity and energy output increases

as well. On the other hand, the chemical activity increases at higher temperatures and could cause a phenomenon called self-discharge which may cause a net loss of capacity [2]. The durability of the battery is also affected by the operating temperature. At low temperatures Li-ion batteries suffer from lithium plating of the anode causing a permanent reduction in capacity. At the upper extreme, the active chemicals may break down destroying the battery. Therefore, battery temperature should be maintained within an appropriate temperature range to guarantee both performance and durability which are critical in HEV applications.

The battery temperature is controlled by the battery thermal management system (BTMS). Thus, the primary function of the BTMS is regulating the battery temperature within a desired range. Another function is reducing battery cell to cell temperature variation in a battery pack to avoid unbalancing, and reduced performance. A battery pack in HEVs consists of tens or hundreds of

* Corresponding author. Tel.: +82 2 320 1633; fax: +82 2 322 7003.

E-mail addresses: parksj@hongik.ac.kr (S. Park), dohoy@umich.edu (D. Jung).

¹ Tel.: +1 313 436 9137; fax: +1 313 593 3851.

individual cells connected in series due to the small rated voltage of a battery cell. Thus, uneven temperature distribution is one of the causes of an unbalanced battery pack [3]. The unbalanced battery pack results in additional power consumption and complexity of the system. Thus, the BTMS should minimize the cell to cell temperature variations in a battery module/pack.

A battery thermal management system can be configured in different architectures and either the air or a liquid can be used as a heat transfer fluids (HTFs). Since the maximum allowable operating temperature of the battery is much lower than those of the power train components the battery is typically cooled using the ambient air or the cabin air chilled by the air conditioning (AC) system in air type system. In a liquid type system a liquid coolant is conditioned using a heat exchanger and the coolant is delivered to the battery pack by a dedicated cooling circuit. The air type system is simpler in design, less expensive, and easier to maintain. Its warm-up period is shorter than the liquid type system which has larger thermal inertia with the liquid coolant in the system. However, the air is not an efficient heat transfer fluid due to relatively lower heat capacity and heat transfer rate than liquids. Battery thermal management using a liquid is more effective and efficient especially for a vehicle with a larger battery pack. A liquid system can reduce the overall system size due to higher heat transfer coefficient. The pumping power consumption is also less than that of air type BTMS. Due to the significant differences in thermal properties of HTFs, the architectural design of a BTMS such as circuitry, configuration, component size, and battery cell arrangement in the pack should be optimized for the specific HTF type.

There have been studies on the design of the BTMS. Pesaran et al. have studied various methods of BTMS and compared air type and liquid type [1,4]. They concluded that air type BTMS is adequate for the parallel HEVs and liquid type BTMS may be required for series HEVs and Electric Vehicles (EVs). Park and Jaura developed a dynamic BTMS model for a battery module and validated the model with experimental data [5]. Ma et al. also modeled the thermal management of battery module using CFD and tried to find the routes of the heat rejection from the Li-ion battery module [6]. Recently, Sun et al. studied the effect of air duct shape on the cell to cell variation of the battery module by using CFD [7]. However, since these studies are using CFD which requires intensive calculation, the model cannot be used for the parametric studies of BTMS design.

Even though there have been many researches on the design of BTMS using numerical modeling and simulation. Most of the researches on the BTMS are limited to the modeling and simulation of a single cell or a battery module and little attention has been paid to the auxiliary components of the BTMS including pump, fan, and heat exchanger and the architectural design of the BTMS depending on the HTF from the viewpoint of the entire system.

In this study, numerical models of a typical air type system and a liquid type system are developed and the effects of the battery cell arrangement and heat transfer fluid on the battery cooling performance and the parasitic power consumption of the BTMS are investigated to provide design guidelines for effective and fuel-efficient battery thermal management. A cylindrical Li-ion battery cell is selected and the battery module size is determined based on the capacity of the battery pack suitable for a passenger car. Figs. 1 and 2 show the configurations of the systems modeled in this study. As shown in the figures, the BTMS model consists of battery cells, battery modules, a pump, a fan, and a heat exchanger. A comprehensive BTMS model developed in this study includes 1-D model for each battery cell, 1-D model for battery module, and 2-D model for the heat exchanger. Although the model developed in this study cannot predict multi-dimensional characteristics of the coolant

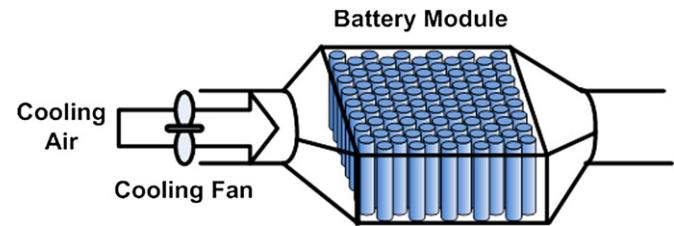


Fig. 1. Configuration of air type BTMS.

flow and heat transfer in the battery module, it is computationally efficient for the system analysis and parametric study of BTMS considering the simulation time and cost compared with CFD model. Parametric studies are conducted using the model, by varying the cell arrangement in the battery module and HTF passage gap for air and liquid type systems with the constraints on the maximum cell temperature and the maximum cell to cell variation.

2. Modeling method

2.1. One-dimensional thermal model for a cylindrical battery cell

In a cylindrical Li-ion battery cell the core temperature of the cell is higher than the surface temperature and the core temperature should be controlled lower than the temperature limit as well as the surface temperature. To predict the core temperature and the in-cell temperature distribution, a one-dimensional thermal model is developed using a finite difference method. The temperature is assumed to vary mainly in the radial direction because the thermal conduction in the radial direction of a spirally wound Li-ion battery is much higher than the axial direction [8]. Thus, the temperature along the cylinder axis is assumed to be uniform. It is also assumed that the heat transfer on the top and bottom surfaces of cylindrical battery is negligible compared with the heat transfer on the side surface with the coolant.

The following heat conduction equation in a long cylinder with a heat generation is used in this study [9,10].

$$\frac{1}{\alpha} \frac{\partial T}{\partial t} = \frac{\partial^2 T}{\partial r^2} + \frac{1}{r} \frac{\partial T}{\partial r} + \frac{\dot{g}}{k} \quad (1)$$

where T is the temperature, \dot{g} is the heat generation rate which is assumed to be uniform in the battery cell, α is the thermal diffusivity, and k is the thermal conductivity of the battery.

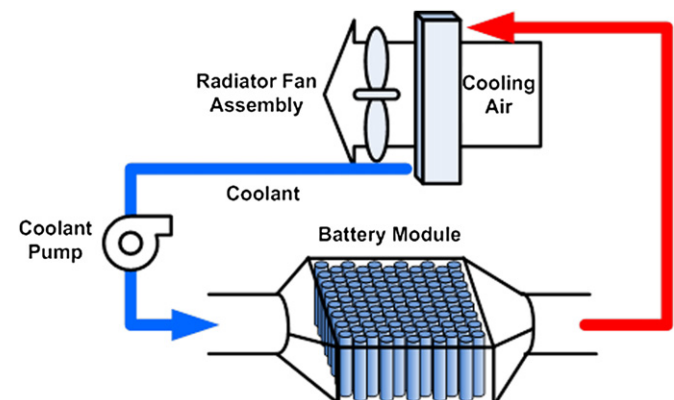


Fig. 2. Configuration of liquid type BTMS.

Heat is generated in a cell due to the irreversible joule heating, the reversible entropic losses, the side reaction, the corrosion reaction, and the parasitic losses. In this study, only the irreversible portion of the heat generation is considered because of the relatively high charge/discharge rate in the HEV application [11]. Accordingly, the heat generation rate per unit volume in a cell is

$$\dot{g} = \frac{i^2 R}{\left(\frac{1}{4}\pi D^2 L\right)} \quad (2)$$

where i is the current in a cell, R is the internal resistance, and D and L are the diameter and the length of the cell respectively.

The boundary condition for the core line is the adiabatic condition:

$$\frac{\partial T}{\partial r} = 0 \quad \text{at } r = 0 \quad (3)$$

The boundary condition for the outer surface is the convective heat transfer to the HTF:

$$-k \frac{\partial T}{\partial r} = h(T - T_\infty) \quad \text{at } r = \frac{1}{2}D \quad (4)$$

where h is the convective heat transfer coefficient on the surface of the battery cell. The heat transfer coefficient is calculated from the battery array model at each column of the battery cells as described in the next section.

2.2. Heat transfer model for a battery array

The battery cells are connected in series to deliver the high power required to drive a vehicle. Thus, a number of cells are arranged with a gap between cells in a battery module. To investigate the design effect of the battery arrangement in a module on the thermal management, the heat transfer and the pressure drop models are developed for a battery module. The model predicts the cell to cell temperature variation and the flow resistance in a module and the power consumption of the cooling fan/pump.

The heat transfer between the battery cell and the HTF is affected by the design parameters and the operating condition such as heat generation, temperatures and flow rate of the HTF. The design parameters of a staggered type battery arrangement are shown in Fig. 3. The convective heat transfer coefficient between the battery cell and the HTF is given by

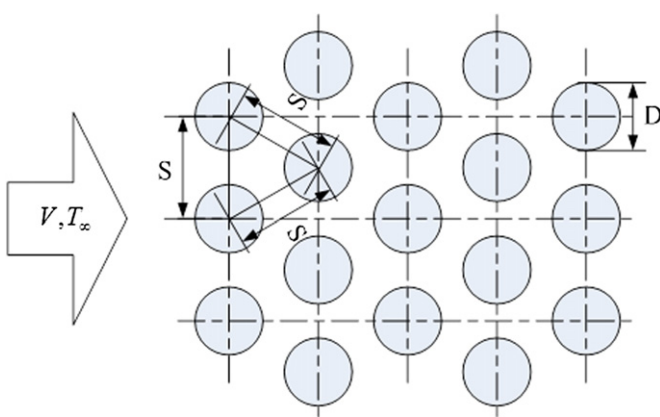


Fig. 3. Schematic of the battery array (bank) and the design parameters of the battery array (bank).

$$h = \frac{D\bar{N}u_D}{k_c} \quad (5)$$

where k_c is the thermal conductivity of the HTF.

The Nusselt number ($\bar{N}u_D$) correlation is adopted from the model developed by Zhukauskas and Ulinskas [12]:

$$\bar{N}u_D = \begin{cases} 0.9Re_{D,\max}^{0.4}Pr^{0.36}\left(\frac{Pr}{Pr_s}\right)^{1/4} & \text{for } 10 < Re < 100 \\ 0.51Re_{D,\max}^{0.5}Pr^{0.36}\left(\frac{Pr}{Pr_s}\right)^{1/4} & \text{for } 100 < Re < 1000 \\ C0.35Re_{D,\max}^{0.4}Pr^{0.36}\left(\frac{Pr}{Pr_s}\right)^{1/4} & \text{for } 1000 < Re < 2 \times 10^5 \end{cases} \quad (6)$$

The Reynolds number $Re_{D,\max}$ in Eq. (6) is defined as

$$Re_{D,\max} = \frac{V_{\max}D}{\nu} \quad (7)$$

where ν is the dynamic viscosity, and V_{\max} is the maximum flow speed in the battery bank which occurs at the gap between the cells in Fig. 3. V_{\max} is calculated from

$$V_{\max} = \frac{S}{S-D}V \quad (8)$$

Correction factor C in Eq. (6) is listed in Table 1.

2.3. Pressure drop model for a battery module

A cooling fan or a pump which supplies the HTF to the battery module causes the parasitic power consumption. The power consumption is calculated based on the volume flow rate, pressure drop in the HTF circuit, and the efficiency of the fan or the pump. The pressure drop occurs due to the frictional resistance in the pipes/ducts (Δp_{pipe}), the expansion and contraction losses at the inlet and the exit of the module ($\Delta p_{\text{exp,cont}}$), and the flow restriction in the battery array (Δp_{bank}) as illustrated in Fig. 4. The power consumption of a fan/pump is formulated as

$$W = \dot{V}(\Delta p_{\text{pipe}} + \Delta p_{\text{exp,cont}} + \Delta p_{\text{bank}}) / \eta_{\text{fan/pump}} \quad (9)$$

where \dot{V} is the volume flow rate of HTF.

The pressure drop in the pipe or duct in Eq. (9) is calculated by

$$\Delta p_{\text{pipe}} = f\left(\rho \frac{V^2}{2}\right) \quad (10)$$

The friction factor f is found from the Moody diagram [13] depending on the Reynolds number and the pipe roughness. The pressure drop induced by the sudden expansion and contraction of the flow path in Eq. (9) is calculated by

$$\Delta p_{\text{exp,cont}} = K_{\text{exp,cont}}\left(\rho \frac{V^2}{2}\right) \quad (11)$$

The contraction and expansion loss coefficient $K_{\text{exp,cont}}$ is found from a Ref. [14].

Table 1

Correction factor C in Eq. (6) ($Re_D > 1000$).

Number of columns	1	2	3	4	5	7	10	13	16
Correction factor (C)	0.64	0.76	0.84	0.89	0.92	0.95	0.97	0.98	0.99

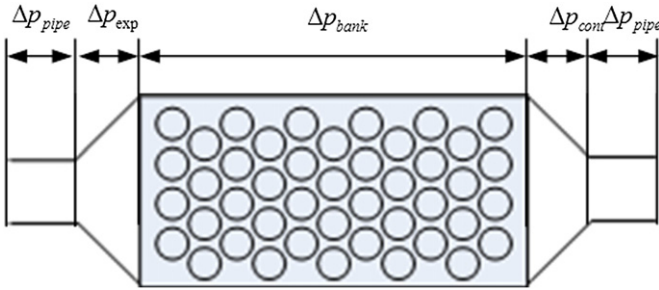


Fig. 4. The pressure drops modeled in the model of the battery module.

The pressure drop in the battery array in Eq. (9) is calculated using the Zukauskas' correlation [15]:

$$\Delta p_{\text{bank}} = N_L X \left(\rho \frac{V_{\text{max}}^2}{2} \right) f \quad (12)$$

where N_L is the number of columns of the battery module and X and f are the pressure drop coefficients which are found in Ref. [15].

3. Results and discussion

3.1. Validation of battery cell model

The one-dimensional thermal model of a cell is validated with an experimental data from Forgez et al. [10]. They measured the surface and the core temperatures of a single cell with thermocouples installed on the outer surface and in the core of a cylindrical Li-ion battery. The specifications of the battery cell are listed in Table 2. Using the results, the model of the cylindrical battery cell is validated with the experimental results as shown in Fig. 5.

3.2. Effect of the BTMS design parameters on the performance and the parasitic power consumption

3.2.1. BTMS design setup for parametric studies

To determine the number of the cells and modules in a battery pack, the battery pack voltage and the capacity are selected as 280 V and 1.8 kWh referring to the nominal values of hybrid electric cars in the U.S. market. In general, the number of cells in a module is determined by the operating voltage of the power electronics and the number of modules in the pack is determined by the required capacity of the battery. Based on the nominal voltage of the Li-ion battery cell (Table 2), 88 cells of Li-ion battery are connected in series to make 280 V in a module. 3 modules are needed to meet the power required for the baseline HEV (1.8 kWh). Table 3 summarizes

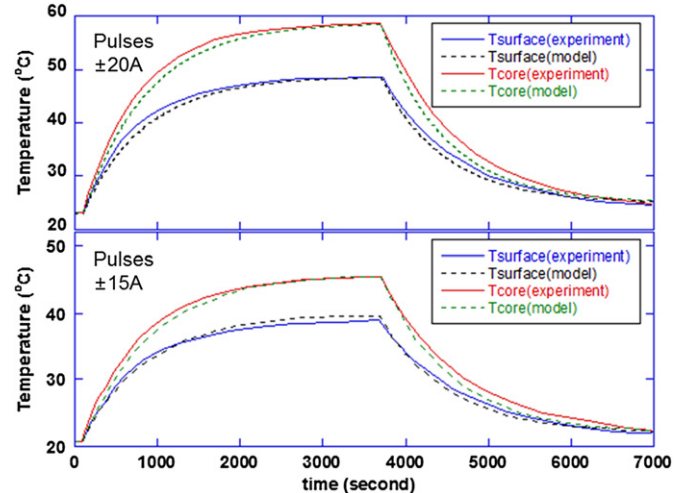


Fig. 5. Validation of cylindrical battery cell model (current pulse ± 20 A and ± 15 A at 2 Hz frequency is applied for 3600 s in the air with an ambient temperature of 22 °C).

the specifications of the battery pack selected for parametric studies.

The heat generated from the battery pack varies depending on the driving condition. Therefore, the range of heat generation during a driving cycle was estimated to fix the design of BTMS prior to the parametric study. The average and peak heat generations from the battery cell under a driving cycle are estimated from the results of a numerical study by Zolot et al. [16]. They configured a vehicle model based on the specifications of a hybrid electric car and simulated battery power profile under US06 driving cycle. The simulation result shows that the battery power profile peaks up to 25 kW and the average power is 3.2 kW during the driving cycle. The heat generation from a battery cell, Q , can be estimated from

$$Q = i_c^2 R_c = i_m^2 R_c = \left(\frac{P}{V_m N_m} \right)^2 R_c \quad (13)$$

where i_c is the current per battery cell, R_c is the internal resistance of the cell, i_m is the current per module, P is the battery pack power, V_m is the nominal battery module voltage, and N_m is the number of modules in the battery pack. The average and peak heat generations by a battery cell calculated using Eq. (13) with the average and peak power over the driving cycle are 0.12 W/cell and 7.01 W/cell, respectively. Using these values as the range of heat generation, the parametric study is conducted for the air cooling and liquid cooling systems.

The battery temperature is managed by changing the HTF flow rate. The HTF flow rate is controlled in such a way that the maximum cell temperature and the maximum cell to cell temperature variation in a module are lower than desired limits. 60 °C is selected as the maximum cell temperature considering the safety

Table 2
Specifications of LiFePO₄/graphite lithium-ion battery (ANR26650M1-A manufactured by A123 systems).

Dimension	
Diameter (mm)	26
Height (mm)	65
<i>Thermal properties</i>	
Thermal conductivity (W m ⁻¹ K ⁻¹)	0.355
Heat capacity [mC _p] (J K ⁻¹)	77.7
<i>Electronic performance</i>	
Nominal voltage (V)	3.3
Nominal capacity (A h)	2.3
Internal resistance (mΩ)	8

Table 3
Specifications of battery pack for light duty passenger HEVs.

Battery cell	LiFePO ₄ /graphite lithium-ion battery (ANR26650M1-A A123 systems)
Number of cells/module	88
Number of modules	3
Total number of cells	264
Nominal battery pack voltage (V)	282
Nominal battery capacity (kWh)	1.94

limit of a Li-ion battery and 3 °C is selected as the maximum cell to cell temperature variation based on the requirement for the HEV batteries and the margin for the transient fluctuation of the temperature [5]. In a battery module, the temperature of the battery cells at the exit of the HTF is the highest and the core temperature is higher than the surface temperature within a cell. Therefore, the core temperature of the last cell (at the exit of the HTF) in a module is maintained under 60 °C by controlling the HTF flow rate. The temperature difference between the first cell and the last cell in a module is also monitored and managed to limit the maximum difference under 3 °C by the control of the HTF flow rate.

3.2.2. Design and parametric studies of air type BTMS

In this case study, the battery pack consists of three battery modules. Thus, it is assumed that three battery modules are cooled by each cooling fan for each module. The cooling fan induces the air from the cabin and blows the air through the cooling passage in the module. It is also assumed that the temperature of the cabin air which is used for the battery cooling is maintained at 25 °C by the AC system. A parametric study is conducted to investigate the effect of design parameters on the performance and power consumption of the system. Selected design parameters are defined in Fig. 6 and the ranges of the parameters are summarized in Table 4.

First parameter investigated in this study is the aspect ratio of the battery module. Fig. 7 shows the effect of the aspect ratio on the BTMS power consumption (Cooling fan power consumption). The BTMS should fulfill two cooling requirements; the maximum temperature and the cell to cell temperature variation. Fig. 7 shows the trends of the power consumption with the aspect ratio change of the battery module controlling the battery temperature based on different cooling requirements.

As the BTMS is controlled to maintain the maximum temperature lower than 60 °C (the line marked with circle in Fig. 7), the power consumption of the BTMS is minimized at the aspect ratio of 0.73. This is due to the different trends of the pressure drops in each part shown in Fig. 4 in the battery module. The BTMS power consumption can be decomposed into three parts to overcome:

- the pressure drops due to the friction in the inlet and exit ducts
- the pressure loss due to the expansion of the flow path at the inlet of the battery module and the contraction of the flow path at the exit of the battery module
- the pressure loss due to the flow resistance in the battery array

The power consumption due to the flow resistance in the battery array is smaller in a wider battery array (high aspect ratio) because of shorter flow path in the battery array, and vice versa in a narrower battery array (low aspect ratio). However, wide battery

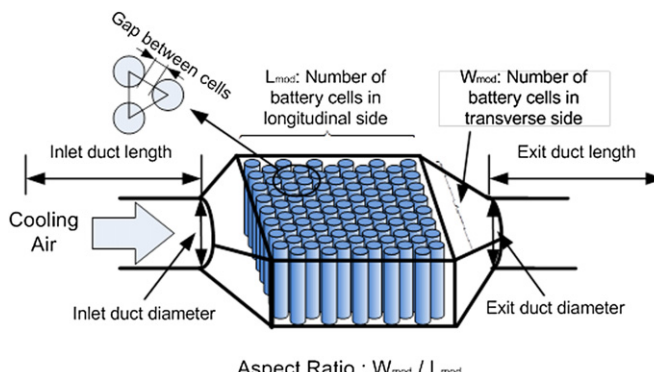


Fig. 6. Definitions of the parameters of air type BTMS.

Table 4
Design parameters of air type BTMS and matrix of parametric study.

Design parameters	Parametric study matrix
Battery cell array arrangement ($L_{\text{mod}} \times W_{\text{mod}}$) and aspect ratio in parenthesis	4 × 22 (0.18), 8 × 11 (0.73), 11 × 8 (1.38), 22 × 4 (5.5)
Inlet/exit duct diameter (mm)	101.6/101.6
Gap between cells (D : cell diameter)	0.25D, 0.5D, 1.0D
Heat generation (W/cell)	3, 5, 7
Inlet/exit duct length (m)	1/1

array requires more air flow due to the increased flow area. Accordingly, the air speed in the duct is higher in wider battery array resulting in higher pressure loss in the duct, and vice versa in a narrower battery array. Wide battery array also results in higher pressure loss at the inlet and exit of the module due to larger changes of flow area, and vice versa in a narrow battery array. In consequence the total power consumption shows a trade-off among the pressure losses and shows minimum power consumption at the aspect ratio of 0.73 (the line marked with circle in Fig. 7).

Fig. 7 also shows the BTMS power consumption with the change of the aspect ratio when the BTMS is controlled to maintain the cell to cell temperature variation lower than 3 °C (the line marked with rectangle in Fig. 7). Wide battery array (high aspect ratio) is desirable for the minimization of the cell to cell temperature variation because the cooling path is short resulting in smaller temperature rise through the cooling path. Therefore, the BTMS with a wide battery array consumes less power to maintain the cell to cell temperature variation lower than 3 °C, and vice versa in a narrow battery array (low aspect ratio). Thus, wide battery array consumes less power as shown in Fig. 7 (the line marked with rectangle in Fig. 7).

Finally, the required power consumption to meet both constraints is plotted with dashed line in the figure, which shows that the optimal aspect ratio is 0.73.

Another design parameter investigated in this study is the gap between the battery cells. Smaller gap is preferable for the packaging, thus, a compact battery module with a small gap is desirable maintaining thermal management system performance. Fig. 8 shows the power consumption changes with the gap and the aspect ratio. Each case shows trend similar to the results shown in Fig. 7. The results suggest that smaller gap requires wider battery array to minimize the power consumption. This is because

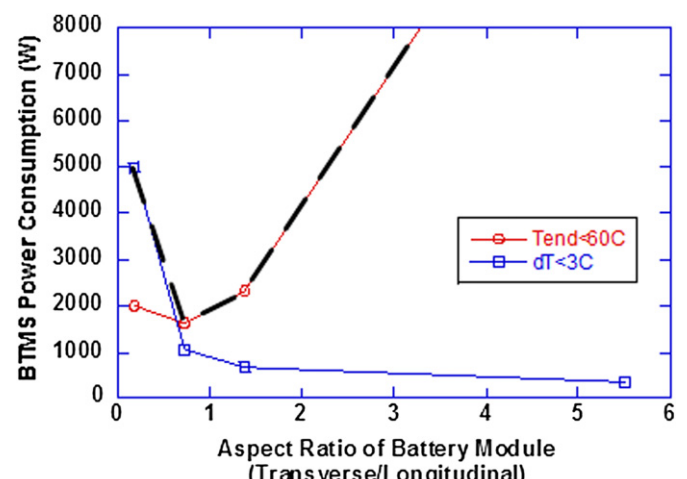


Fig. 7. Effect of aspect ratio of battery module on the power consumption of cooling fan ($Q = 7 \text{ W/cell}$, gap = $1.0D$).

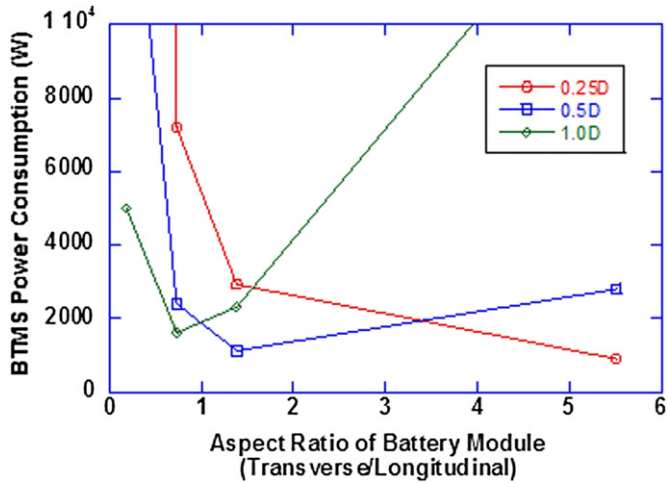


Fig. 8. Effect of gap between the battery cells in a module ($Q = 7 \text{ W/cell}$).

excessive power is consumed for the small gap (small cross section of the cooling path) to minimize the cell to cell temperature variation due to the increase of the coolant temperature as the coolant flows through the cooling path. Thus, wide battery array which has short cooling path can minimize the coolant temperature rise through the battery cooling path. Thus, it can be concluded that a wide battery array is required for the compactness of the battery module.

Cooling air is not a limitless resource because it is supplied by the AC system. The AC system cools down the outer air or recirculated air and supplies the cold air into the cabin to maintain the cabin temperature at an acceptable range. In this study, the cabin air is assumed to be controlled at 25°C by the AC system and the cabin air is used as the coolant for the BTMS. Fig. 9 shows the cooling air flow rate required to cool down the battery pack. The result shows that small gap design spends less cooling air from the cabin. One thing to note here is that the air flow induced from the cabin into the battery pack should be limited because too much air flow from the cabin would make the passenger in the cabin uncomfortable. Thus, the cooling air flow rate of a passenger HEV is a good reference. For example, the maximum cooling air flow rate given in Ref. [16] is $0.36 \text{ m}^3 \text{ s}^{-1}$ (48.4 scfm). Considering the maximum cooling air flow rate, the air type BTMS designed for this

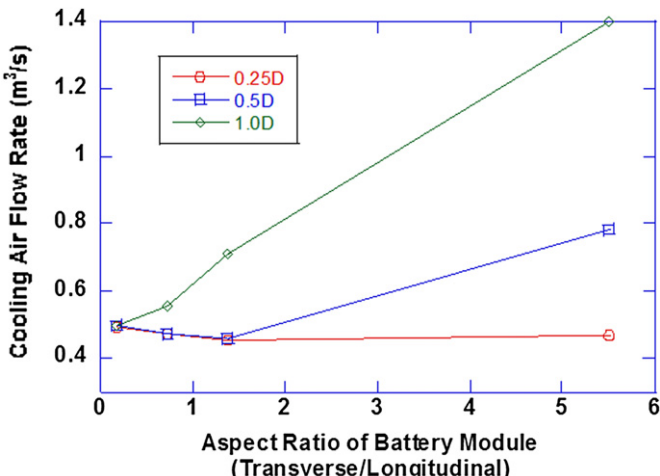


Fig. 9. Effect of aspect ratio of battery module on the flow rate of cooling air ($Q = 7 \text{ W/cell}$).

case study requires too much cooling air as shown in Fig. 9. It is because the BTMS is designed at peak heat generation point ($Q = 7 \text{ W/cell}$). Thus, air flow rate should be taken into consideration for the optimal design of the BTMS for HEVs.

In summary, a wide battery module with a narrow gap is preferable for the design of an air cooled battery module because the power consumption and the flow rate of the cooling air are minimized.

3.2.3. Design and parametric studies of liquid type BTMS

The configuration of liquid type BTMS is different from that of air type BTMS because the system requires additional cooling circuit for the heat exchange between the air and the HTF. Mineral oil is used as the HTF to avoid any electrical shorts in this case study. In the liquid type BTMS shown in Fig. 2, the liquid (mineral oil) cools the battery cells directly flowing between the battery cells in a battery module and the liquid is cooled by the cooling air in a radiator fan assembly. The cooling air is assumed to be induced from the cabin and the temperature is assumed to be 25°C . Generally, a radiator is used for the heat exchange between the air and liquid because the heat transfer coefficient for air side is much lower than that for liquid side. Thus, low heat transfer coefficient is supplemented by the increased heat transfer area in the radiator. 2-D Finite Difference Method (FDM) Model developed by Jung and Assanis [17] is used for the radiator model because the heat transfer and power consumption in the radiator and fan assembly are critical parts of the BTMS analyses. The 2-D model can predict the effect of detailed design of the radiator on the heat exchange performance and pressure drop in the coolant flow path. Park and Jung developed comprehensive vehicle cooling system model including pump, fan, and radiator assembly [18]. The models are integrated with the BTMS model to predict the system response of the liquid type BTMS. Using the model, parametric study is conducted to evaluate the effect of design parameters on the performance of the BTMS. The design parameters selected for the liquid type BTMS and the range of the parameters are summarized in Table 5. In the liquid type BTMS, a large size radiator is preferable to minimize the power consumption because the heat transfer rate is proportional to the heat exchange area. However, the radiator size is limited by the packaging space of the battery system in a HEV. In this study, the radiator size is determined considering the battery module size assuming that the BTMS is integrated with the battery modules for the compactness of the system which is listed in Table 5.

Fig. 10(a) shows the effect of the air flow rate change on the oil flow rate and cell to cell variation. In all cases, the core temperature of last cell in the battery module is controlled at 60°C by changing the oil flow rate. As shown in the figure, at low air flow rate, the BTMS requires high oil flow rate to supplement the heat transfer rate. The cell to cell temperature variation in the battery module is also affected by the air flow rate change as shown in Fig. 10(a). The

Table 5

Design parameters of liquid type BTMS and matrix of parametric study.

Design parameters	Parametric study matrix
Battery cell array arrangement ($L_{\text{mod}} \times W_{\text{mod}}$, aspect ratio defined in Fig. 6))	$22 \times 4 (0.18), 11 \times 8 (0.73), 8 \times 11 (1.38), 4 \times 22 (5.5)$
Inlet/exit pipe diameter (mm)	50.8/50.8
Gap between cells (D : cell diameter)	$0.02D, 0.03D, 0.05D, 0.1D$
Heat generation (W/cell)	5, 7
Inlet/exit pipe length (m)	1/1
Radiator size (Width (m) \times Height (m))	0.5×0.2
Radiator thickness (mm)	30
Cooling air flow rate ($\text{m}^3 \text{ s}^{-1}$)	0–1.0

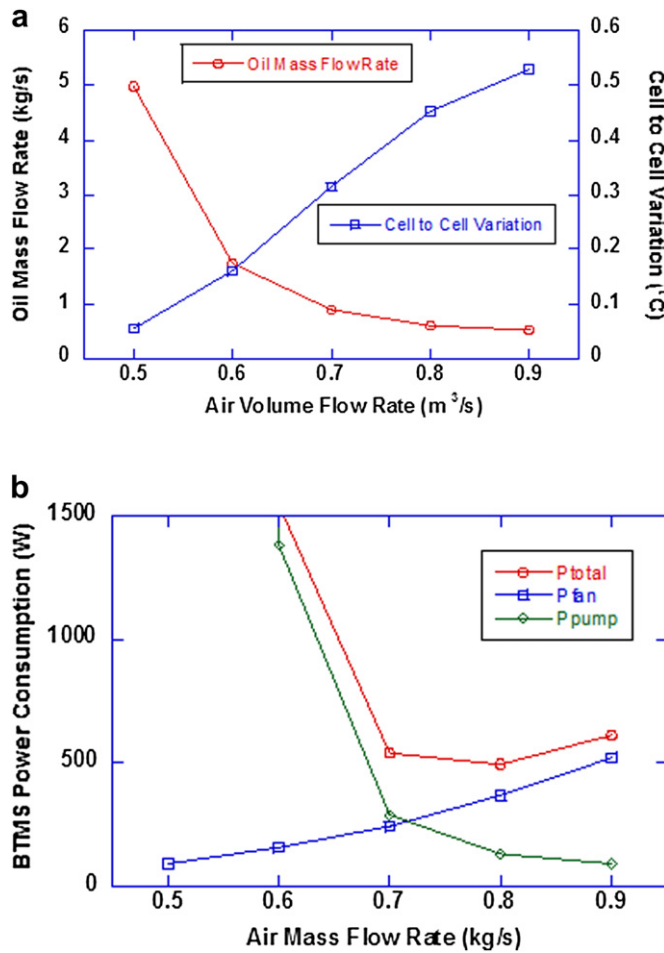


Fig. 10. Effect of air volume flow rate on cell to cell variation and power consumption (aspect ratio: 0.73, gap = 0.03D, $Q = 7$ W/cell, $T_{max} = 60$ $^{\circ}C$).

cell to cell temperature variation of the battery module is mainly due to the temperature change of the coolant in the battery module. As the coolant flows through the cooling path in a battery module, the coolant temperature increases and the coolant temperature change results in the cell to cell temperature variation in the battery module. Thus, the cell to cell temperature variation is reduced when a large amount of coolant is supplied to the module because large coolant supply results in small temperature increase of the coolant in the module. Thus, as the air flow rate increases, less oil is circulated to the battery module to maintain the heat transfer rate, as a result, the cell to cell temperature variation increases due to low oil flow rate in the module as shown in Fig. 10(a).

Fig. 10(b) shows the effect of the air flow rate change on the power consumption of the BTMS including cooling pump and fan. As can be seen in the figure, there exists an operating point of the BTMS where the power consumption is minimized due to the different trends of the power consumption of the cooling fan and the pump.

In order to compare the design (aspect ratio and gap between cells) of the liquid type BTMS, optimal operating points including air and liquid flow rates should be determined for each design point. Fig. 11 shows how the optimal BTMS operating point of air and oil flow rate are found at each design point. Fig. 11 is an example of simulation results for the battery module of 22 columns by 4 rows with 0.03D gap. All the points in Fig. 11 satisfy temperature limit (60 $^{\circ}C$). Thus, the optimal operating point can be found

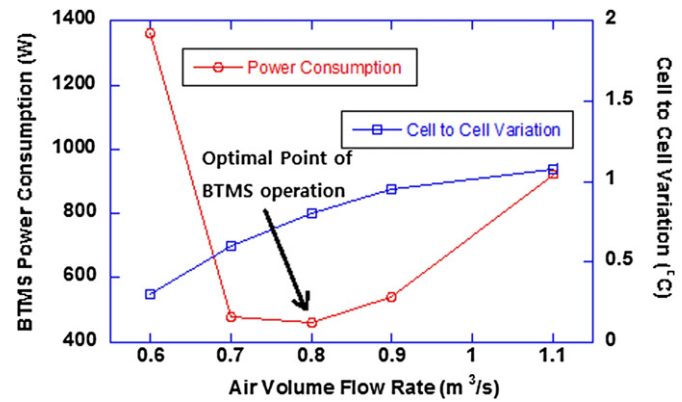


Fig. 11. Effect of aspect ratio of battery module on power consumption and cell to cell variation (22 columns, 4 rows, aspect ratio = 0.18, gap = 0.03D, $Q = 7$ W/cell, $T_{max} = 60$ $^{\circ}C$).

at lowest power consumption point (air volume flow rate = 0.8 m^3 s^{-1}). However, additional cooling requirements should be fulfilled. First, the cell to cell temperature variation should be lower than the limit (3 $^{\circ}C$). Next, the air flow rate should be lower than the maximum limit. Based on this procedure, the optimal operating point (oil and air flow rates) is found for each design point (aspect ratio and gap) and the results are used for the parametric studies described below.

First, a parametric study on the aspect ratio of the battery module and the gap between the battery cells are conducted to find the impact of the design parameters on the power consumption and the cell to cell variation. The gap between cells is a design parameter that affects the size, weight, warm-up period, and performance of the BTMS. Aspect ratio of the battery module also affects the power consumption and the cell to cell variation. Thus, various sizes of gap and aspect ratio of a battery module are examined to find the impact of the design parameters on the power consumption and the cell to cell variation. Fig. 12 shows the effect of the gap between the cells on the power consumption of the BTMS. Each point is found by the procedure explained above. First observation from Fig. 12 is that, in a narrow battery module (lower aspect ratio) with small gap consumes less power compared with wide battery module with large gap primarily due to the low coolant flow rate. Small gap is advantageous for the weight and packaging of the battery pack. However, wide battery module with

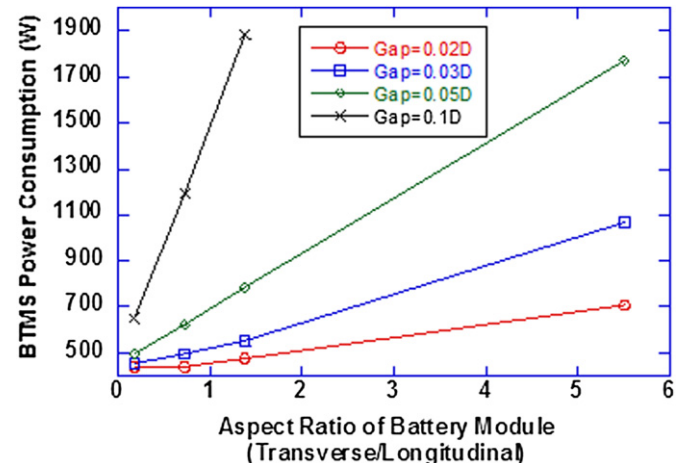


Fig. 12. Effect of gap between battery cells on the power consumption of the BTMS ($Q = 7$ W/cell, $T_{max} = 60$ $^{\circ}C$, $dT < 3$ $^{\circ}C$).

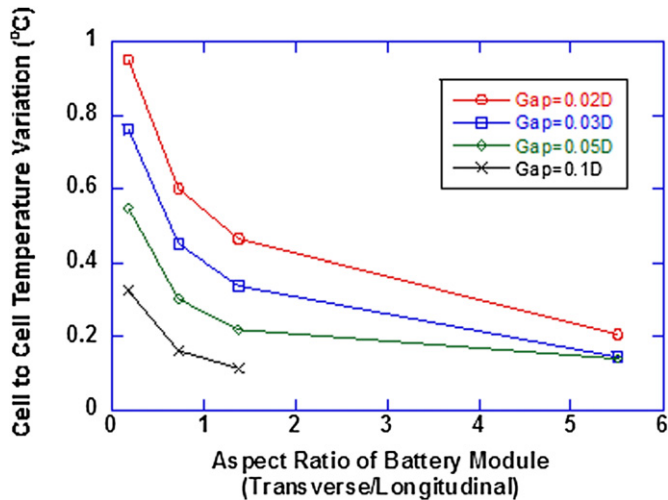


Fig. 13. Effect of gap between battery cells on the power consumption of the BTMS ($Q = 7 \text{ W/cell}$, $T_{\max} = 60 \text{ }^{\circ}\text{C}$, $dT < 3 \text{ }^{\circ}\text{C}$).

Table 6
Comparison of the power consumption of the air type BTMS and liquid type BTMS.

Heat load (W/cell)	Power consumption of air type BTMS (W)	Power consumption of oil cooling BTMS (W)
3	29	—
5	260	28
7	908	445

large gap is advantageous for smaller cell to cell variation. As can be seen in Fig. 13, cell to cell temperature variation is not an issue in the liquid type BTMS because the cell to cell variation is much smaller than the limit ($3 \text{ }^{\circ}\text{C}$). This is because the temperature rise of the HTF through the cooling path in the battery array is very small due to high heat capacity of the liquid HTF. Thus, it can be concluded that a narrow battery module with a small gap is preferable for the liquid type BTMS.

3.2.4. Comparison between air type BTMS and liquid type BTMS

Based on the results of the parametric studies with the air and the liquid type BTMS models, the power consumptions are compared in Table 6. The liquid type BTMS consumes much less power compared with the air type BTMS mainly due to the better thermal properties of liquid and better heat exchange efficiency of the radiator compared with the direct air type BTMS. However, at low heat load conditions, the power consumption and the air flow rate are acceptable because, although the power consumption is still bigger than the liquid type, it has many advantages over the liquid type such as simple design, lower cost, easier maintenance, and shorter warm up period.

4. Summary and conclusions

Battery thermal management system models are developed for an air and a liquid type BTMSs. The parametric studies on the BTMS design for battery module with cylindrical Li-ion battery cells are conducted using the model. The followings are the conclusions from the numerical analysis of the air type BTMS design.

1. The different trends of the power consumptions due to the pressure drops in the duct, expansion and contraction, and

battery array result in an optimal point of the aspect ratio of the battery module.

2. A wide battery array is beneficial to minimize the cell to cell temperature variation while it requires excessive cooling air flow rate resulting in high power consumption.
3. To minimize the power consumption of the BTMS, a small gap between battery cells requires wide battery module and large gap requires narrow battery module.

In summary, a wide battery module with small gap is preferable for the design of a battery module because the power consumption and the flow rate of the cooling air are minimized by the design.

The followings are the conclusions from the numerical analysis of the liquid type BTMS design.

1. There exists operating points where the power consumption of the BTMS is minimized due to the different trends of the flow rates of the cooling air and the liquid to meet the cooling requirements.
2. A narrow battery module with a small gap consumes less power than a wide battery module with a large gap primarily due to the low coolant flow rate. On the other hand, wide battery module with large gap is preferable to minimize the cell to cell variation.

Based on the observations from the numerical design analysis of air and liquid type BTMSs, the air type BTMS consumes much more power compared with the liquid type BTMS. However, at low heat load conditions, the power consumption of the air type BTMS is acceptable because the power consumption of the air type BTMS is comparable to that of the liquid type BTMS and it has many advantages over liquid type BTMS.

Acknowledgments

This work was supported by the Hongik University new faculty research fund.

References

- [1] A.A. Pesaran, in: Advanced Automotive Battery Conference, Las Vegas, Nevada, 2001.
- [2] D. Linden, T.B. Reddy, McGraw-Hill, New York, 2001.
- [3] C. Speltino, D.D. Domenico, G. Fiengo, A.G. Stefanopoulou, in: American Control Conference, AACC, Baltimore, Maryland, 2010.
- [4] A.A. Pesaran, Journal of Power Sources 110 (2002) 377–382.
- [5] C. Park, A.K. Jaura, SAE 2003-01-2286, 2003.
- [6] Y. Ma, H. Teng, M. Thelliez, SAE 2010-01-2204, 2010.
- [7] H. Sun, B. Tossan, D. Brouns, SAE 2011-01-1368, 2011.
- [8] T.I. Evans, R.E. White, Journal of Electrochemical Society 136 (1989) 2145–2152.
- [9] S.A. Hallaj, H. Maleki, J.S. Hong, J.R. Selman, Journal of Power Sources 83 (1999) 1–8.
- [10] C. Forgez, D.V. Do, G. Friedrich, M. Morcrette, C. Delacourt, Journal of Power Sources 195 (2010) 2961–2968.
- [11] K. Smith, C.-Y. Wang, Journal of Power Sources 160 (2006) 662–673.
- [12] A. Zhukauskas, R. Ulinskas, Heat Transfer in Tube Banks in Crossflow, Springer-Verlag, New York, 1988.
- [13] R. Fox, A. McDonald, P. Pritchard, Introduction to Fluid Mechanics, sixth ed., John Wiley, Hoboken, 2004.
- [14] V.L. Streeter, Handbook of Fluid Dynamics, McGraw-Hill, New York, 1961.
- [15] A. Zhukauskas, Advances in Heat Transfer 8 (1972) 93–160.
- [16] M. Zolot, A.A. Pesaran, M. Mihalic, SAE 2002-01-1962, 2002.
- [17] D. Jung, D. Assanis, SAE 2006-01-0726, 2006.
- [18] S. Park, D. Jung, Journal of Engineering for Gas Turbines and Power 132 (2010) 092802-1–092802-11.